OXFORD
SOT | Society of Toxicology
www.toxsci.oxfordjournals.org
ToxSci 20 Years

TOXICOLOGICAL SCIENCES, 164(2), 2018, 428–438

doi: 10.1093/toxsci/kfy106
Advance Access Publication Date: April 27, 2018
Research Article

Alcohol Metabolism in the Progression of Human Nonalcoholic Steatohepatitis

Hui Li, Erica Toth, and Nathan J. Cherrington[1]

Pharmacology and Toxicology, University of Arizona, Tucson, Arizona 85721

[1]To whom correspondence should be addressed at *Pharmacology and Toxicology, University of Arizona*, 1703 East Mabel Street, Tucson, AZ 85721. Fax: (520) 626-2466. E-mail: cherrington@pharmacy.arizona.edu.

ABSTRACT

Alcohol metabolism is a well-characterized biological process that is dominated by the alcohol dehydrogenase (ADH) and aldehyde dehydrogenase (ALDH) families. Nonalcoholic steatohepatitis (NASH) is the advanced inflammatory stage of nonalcoholic fatty liver disease (NAFLD) and is known to alter the metabolism and disposition of numerous drugs. The purpose of this study was to investigate the alterations in alcohol metabolism processes in response to human NASH progression. Expression and function of ADHs, ALDHs, and catalase were examined in normal, steatosis, NASH (fatty) and NASH (not fatty) human liver samples. ALDH4A1 mRNA was significantly decreased in both NASH groups, while no significant changes were observed in the mRNA levels of other alcohol-related enzymes. The protein levels of ADH1A, ADH1B, and ADH4 were each decreased in the NASH groups, which was consistent with a decreased overall ADH activity. The protein level of ALDH2 was significantly increased in both NASH groups, while ALDH1A1 and ALDH1B1 were only decreased in NASH (fatty) samples. ALDH activity represented by oxidation of acetaldehyde was decreased in the NASH (fatty) group. The protein level of catalase was decreased in both NASH groups, though activity was unchanged. Furthermore, the significant accumulation of 4-hydroxynonenal protein adduct in NASH indicated significant oxidative stress and a potential reduction in ALDH activity. Collectively, ADH and ALDH expression and function are profoundly altered in the progression of NASH, which may have a notable impact on ADH- and ALDH-associated cellular metabolism processes and lead to significant alterations in drug metabolism mediated by these enzymes.

Key words: alcohol dehydrogenase; aldehyde dehydrogenase; alcohol metabolism; catalase; nonalcoholic steatohepatitis.

Alcohol metabolism has been extensively studied and is a well-defined process. Over 90% of consumed alcohol is metabolized through the oxidative pathways that are mediated by alcohol dehydrogenase (ADH) and aldehyde dehydrogenase (ALDH) (Lieber, 2005). In this predominant oxidative pathway, alcohol is first oxidized to aldehyde by ADH, followed by ALDH-mediated aldehyde metabolism to acetate. The balance between the various ADH and ALDH isoforms is critical in regulating the cellular concentration of the highly cytotoxic aldehyde (Cederbaum, 2012). Besides alcohol metabolism, ADH and ALDH also participate in other cellular events, such as retinoic acid biosynthesis, folate metabolism, amino acid metabolism, and lipid peroxidation (Vasiliou *et al.*, 2004). Furthermore, it has been reported that ADH and ALDH enzymes play significant roles in the metabolism of numerous clinical drugs (Evans and Relling, 1999). Additionally, ADH and ALDH enzymes can function as the alternative oxidative pathways for several drugs that are primarily metabolized by cytochrome P450s (CYPs) (Strolin Benedetti *et al.*, 2006).

There are 2 alternative pathways that also participate in the oxidation of alcohol to aldehyde in addition to ADH; one is mediated by the microsomal CYPs (mainly CYP2E1), and the other is mediated by peroxisomal catalase (Cederbaum, 2012). Under normal physiological conditions, CYP2E1 only plays a minor role in alcohol metabolism. However, CYP2E1 activity can be significantly induced due to chronic alcohol consumption, and during the CYP2E1 catalytic cycle, significant amounts of reactive oxygen species (ROS) are generated, which may lead to increases in cellular injury, lipid peroxidation, oxidant, and mitochondrial damage, and contribute to various pathological processes (Leung and Nieto, 2013). Catalase, which was first defined as an antioxidant enzyme (Glorieux and Calderon, 2017), can also

catalyze the metabolism of alcohol. The capacity of this reaction is limited, however, by the low level of H_2O_2, and catalase consequently plays only a minor role in the overall metabolism of alcohol (Dinis-Oliveira, 2016).

The majority of alcohol consumed is metabolized through oxidative pathways in the liver (Cederbaum, 2012). Therefore, impaired liver function could have a dramatic impact on the capacity for alcohol metabolism mediated by alcohol metabolizing enzymes. Nonalcoholic fatty liver disease (NAFLD) encompasses a wide spectrum of pathological severity ranging from simple steatosis to nonalcoholic steatohepatitis (NASH), which occurs in the absence of significant daily ethanol consumption (Chalasani *et al.*, 2012). A global epidemic, NAFLD affects about 25% of the world population currently, and its incidence is continuously rising (Younossi *et al.*, 2016). NASH, the most advanced stage of NAFLD, is defined as the presence of primary hepatic steatosis and inflammation with irreversible hepatocellular injury which may progress to fibrosis, cirrhosis, and hepatocellular carcinoma (Vernon *et al.*, 2011). Although disruptions in certain cellular pathways, such as insulin signaling, oxidative stress, endoplasmic reticulum (ER) stress, and autophagic stress, have been recognized as contributing factors in human NASH progression, the molecular mechanisms driving the development and progression of NASH are not fully understood (Chitturi *et al.*, 2002; Gonzalez-Rodriguez *et al.*, 2014; Lake *et al.*, 2014; Takaki *et al.*, 2013). NASH exhibits distinct gene expression signatures, particularly in the genes associated with absorption, distribution, metabolism, and excretion (ADME) processes. In a previous genome-wide study, a profound reprogramming was found in the gene expression of drug metabolizing enzymes and drug transporters in human NASH (Lake *et al.*, 2011). Several subsequent investigations further demonstrated significant alterations in the expression and function of individual phases I and II enzymes and drug transporters (Fisher *et al.*, 2009; Hardwick *et al.*, 2011, 2013). Furthermore, ADME reprogramming in NASH leads to comprehensive alterations in the pharmacokinetic profiles of multiple clinical drugs, which have been observed in both human NASH patients and animal models (Canet *et al.*, 2015; Clarke *et al.*, 2014; Dzierlenga *et al.*, 2015; Hardwick *et al.*, 2014; Li *et al.*, 2017). Besides exogenous compounds, a distinctive profile of endogenous metabolites, including bile acids, amino acids and fatty acids further demonstrate the impact of NASH-associated ADME alterations on metabolism processes (Han *et al.*, 2017).

Alcohol metabolism has been extensively studied in alcoholic fatty liver disease (AFLD) and alcoholic steatohepatitis. However, a comprehensive analysis of alcohol metabolizing enzymes and alcohol metabolism processes in the progressive stages of NAFLD has not been studied in humans. The current study is the first to determine the impact of human NAFLD progression on hepatic alcohol metabolism pathways. These data may be useful in estimating dosing adjustments needed in NAFLD patients taking drugs that are metabolized by these pathways.

MATERIALS AND METHODS

Chemicals and reagents. Hexanal and octanal were purchased from Sigma-Aldrich (St Louis, Missouri). All other chemicals were obtained from commercial sources.

Human liver samples. Postmortem formalin-fixed, paraffin-embedded (FFPE) and frozen adult human liver samples were obtained from the liver tissue cell distribution system (LTCDS) coordinated through the University of Minnesota, Virginia Commonwealth University, and the University of Pittsburgh. Sample diagnosis was first performed by LTCDS and then confirmed by histological examination at the University of Arizona in a blinded fashion. Steatotic liver was diagnosed when >10% of hepatocytes showed fat deposition. NASH (fatty) liver diagnosis was defined as having marked inflammation, fibrosis, and >5% of hepatocytes with fat deposition. NASH (not fatty) liver was diagnosed by marked inflammation, fibrosis, and <5% of hepatocytes with fat deposition. Detailed information of liver samples and donors are included in the Supplementary Table 1 and also were published previously in Fisher *et al.* (2009) and Hardwick *et al.* (2011).

Total RNA isolation and mRNA analysis. Total RNA was extracted from human liver tissues using RNAzol B reagent from Tel-Test Inc. (Friendswood, Texas) according to the manufacturer's protocol. Equal amounts of RNA (1 μg) were used for reverse transcription using the ReadyScript cDNA synthesis mix (RDRT-100RXN, Sigma-Aldrich). The KiCqStart SYBR Green predesigned primers for gene expression analysis were also obtained from Sigma Aldrich (KSPQ12012, primer pair ID: H_ACTB_1, H_ADH1A_1, H_ADH1B_1, H_ADH1C_1, H_ADH4_1, H_ADH5_1, H_ALDH1A1_1, H_ALDH1B1_1, H_ALDH1L1_1, H_ALDH2_1, H_ALDH3A2_1, H_ALDH4A1_1, H_ALDH5A1_1, H_ALDH6A1_1, H_ALDH7A1_1, H_ALDH8A1_1, H_ALDH9A1_1, H_ALDH16A1_1 and H_ALDH18A1_1) (Sigma-Aldrich). Quantitative real-time PCR was performed as follows: 1 cycle of initial denaturation (4 min at 95°C), 45 cycles of amplification (10 s at 95°C and 30 s at 60°C), and a cooling period. The threshold cycle (Ct) value of each sample was obtained from the instrument. The relative mRNA fold of each gene was determined for each sample relative to the endogenous control Actin-beta (delta Ct = Ct_{target}—$Ct_{actin\text{-}beta}$), and the $\log_2$ of fold change of each gene in each disease group was determined as—delta (delta Ct) = —(delta $Ct_{disease}$—delta Ct_{normal}).

Single nucleotide polymorphisms genotyping. Single nucleotide polymorphism (SNP) genotyping was performed for ALDH2 (rs671) and ADH1B (rs1229984). DNA was extracted from human liver tissues and quantified before turned over for normalization and reaction. DNA (25 μl of 5 ng/μl) was made for Taqman reactions and plated into 96-well optical PCR plates. Each well was loaded with 2 μl for a total of 10 ng per genotyping reaction. After DNA was loaded, a master mix was made of Taqman Fast Advance Master Mix (Life Technologies, Carlsbad, California), Taqman SNP Genotyping assay (Life Technologies), and PCR water (Thermo Fisher Scientific, Waltham, Massachusetts) according to the manufacturer's protocols. The master mix was plated into the reaction plate with an 8-channel pipette, sealed, vortexed, and centrifuged, then preread on ABI 7300 instrument (Thermo Fisher Scientific). After pre-reading, the plate was cycled on a Biorad Tetrad PCR cycler. The standard times for the thermal cycling was used, though a step with 58°C anneal/extend hold was used instead of the 60°C from the manufacturer's protocol. After cycling, the plate was centrifuged and postread on the 7300 instrument. The data were generated and analyzed by the ABI 7300 instrument software. Samples from individuals who carried the ALDH2 and ADH1B polymorphisms were excluded from the statistical analysis.

Immunoblot analysis. Human liver tissue (300 mg) was homogenized in NP40 lysis buffer (20 mM Tris-HCl, 137 mM NaCl, 10% glycerol, 1% Nonidet P-40, and 2 mM EDTA) with 1 protease

inhibitor cocktail tablet per 25 ml (Roche, Indianapolis, Indiana) on ice. Homogenized tissue was centrifuged at 10, 000 × g for 30 min, and the supernatant was transferred to a new collection vial. Protein concentrations in the collected supernatant were quantified by the Pierce BCA Protein Quantitation Assay kit (Thermo Fisher Scientific) following the manufacturer's protocol.

Human liver whole cell lysate (40 μg each well) were separated on 10% SDS-PAGE gels and transferred to polyvinylidene difluoride membranes. The following antibodies were used for the detection of proteins: ERK1 (sc-93), ERK2 (sc-154), ADH4 (sc-515217), ALDH1A1 (sc-374149), ALDH1B1 (sc-393583), ALDH2 (sc-100496), ALDH4A1 (sc-398911) (Santa Cruz Biotechnology, Inc., Dallas, Texas), catalase (ab209211) (Abcam, Cambridge, Massachusetts, Ab62204), ADH1A (SAB2100057) and ADH1B (AV41787) (Sigma-Aldrich). Densitometry analysis of the western blot was performed using ImageJ software (National Institutes of Health, Bethesda, Maryland), and relative protein expression was calculated by normalizing to the total ERK (ERK1/2).

Immunohistochemistry. Immunohistochemical (IHC) staining for 4HNE protein adduct was performed with FFPE human liver tissue blocks. Tissue sections were preheated at 50°C for 5 min, and then deparaffinized in xylene and rehydrated in 100% ethanol followed by 70% ethanol. Tris-EDTA buffer (pH = 9) was used for the antigen retrieval. 0.3% (v/v) H_2O_2 in PBS for 20 min. MACH3 staining kit (Biocare Medical, Concord, California) and 4HNE antibody (obtained from Dr Dennis R. Petersen) was used in 4HNE staining. Liver tissue sections were incubated in a primary antibody solution overnight at 4°C. Staining color was developed with the Betazoid DAB (Biocare Medical), and then slides were counterstained with hematoxylin (Sigma-Aldrich). The stained slides were examined and imaged with Nikon Eclipse E4000 microscope and a Sony Exwave DXC-390 camera (Nikon Instruments, Melville, New York). IHC staining analysis was done using Definiens Tissue Studio 4.2 on the entire field of view of the slide images. Tissue Studios's Marker Area Detection feature was used to identify and quantify the percentage of positive 4-HNE protein adduct staining in the images.

ADH, ALDH, and catalase activity assays. According to the manufacturer's protocol, an ADH activity assay kit was used to examine the activity of ADH in ethanol oxidation (E-108), and an ALDH activity assay kit was used to examine the activity of ALDH in acetaldehyde, hexanal and octanal oxidation (E112) (Biomedical Research Service and Clinical Application, Baffalo, New York). Hepatic catalase activity was measured by a Catalase-Specific Activity Assay Kit obtained from Abcam (ab118184).

Statistical analysis. All results are represented as the mean ± SD. For all comparisons within this study 1-way analysis of variance statistical analysis was employed with a Tukey's multiple comparisons posttest to compare normal versus steatosis, NASH (fatty), NASH (not fatty), steatosis versus NASH (fatty), NASH (not fatty), and NASH (fatty) versus NASH (not fatty). All analysis was carried out using GraphPad Prism software (GraphPad Software, Inc., La Jolla, California).

RESULTS

Histology of Human Livers With Progressive Stages of NAFLD

Representative human liver samples with hematoxylin and eosin (H&E) staining are shown in Figure 1. Steatosis liver shows excessive fatty infiltration (>10%). NASH (fatty) samples present macrovesicular fat deposition along with significant hepatic inflammation and fibrosis. The progression to NASH (not fatty) involves a reduction in hepatocellular lipid deposition but a significant expansion of hepatic fibrosis.

Hepatic Expression and Function of ADH Isoforms During the Progression of Human NAFLD

mRNA levels of human ADH1A, ADH1B, ADH1C, ADH4 and ADH5 were assessed by the real-time qPCR in the human liver samples. The box-whiskers plot represents the $\log_2$ of fold change of each gene in normal, steatosis, NASH (fatty) and NASH (not fatty) groups. The mRNA levels of ADH isoforms examined in this study were not significantly altered in human steatosis or NASH livers (Figure 2A). On the contrary, the protein levels of ADH1A, ADH1B, and ADH4 were each significantly decreased in both NASH (fatty) and NASH (not fatty) samples compared with normal and steatosis samples (Figure 2B). Consistently, the overall ADH activity assessed by ethanol oxidation was significantly decreased in both NASH groups compared with normal (Figure 2C).

Hepatic Expression and Function of ALDH Isoforms During the Progression of Human NAFLD

mRNA levels of human ALDH1A1, ALDH1B1, ALDH1L1, ALDH2, ALDH3A2, ALDH4A1, ALDH5A1, ALDH6A1, ALDH7A1, ALDH8A1, ALDH9A1, ALDH16A1, and ALDH18A1 were assessed by the real-time qPCR in the human liver samples, and the box-whiskers plot represent the $\log_2$ of fold change of each gene in normal, steatosis, NASH (fatty) and NASH (not fatty) groups. The mRNA levels of ALDH4A1 were significantly decreased in both NASH groups, while mRNA levels of the other ALDH isoforms remained unchanged (Figure 3A). The protein levels of ALDH1A1 and ALDH1B1 were significantly decreased in the NASH (fatty) but not NASH (not fatty) samples. There is a significant increase in ALDH2 protein level in both NASH groups. ALDH1A1 and ALDH1B1 protein levels are significantly downregulated in the NASH (fatty) group but not NASH (not fatty). ALDH2 protein level is significantly downregulated in both NASH groups (Figure 3B). ALDH activity was measured using acetaldehyde, octanal, and hexanal. NASH (fatty) livers show a decreased ALDH activity against acetaldehyde, but octanal oxidation is significantly increased in steatotic livers. An upward trend is shown in activity toward hexanal, but this was not statistically significant (Figure 3C).

Hepatic Expression and Function of Catalase During the Progression of Human NAFLD

The hepatic protein expression of catalase, assessed by immunoblotting, was significantly decreased in the NASH groups compared with control. The activity of catalase in the liver lysate was determined using a catalase-specific activity assay kit, and no significant change was observed.

4-Hydroxynonenal Protein Adduct Formation in Human NAFLD Progression

An antibody that specifically recognizes 4-hydroxynonenal (4-HNE)-modified proteins was used for the IHC staining of human liver slides. A significant accumulation of 4-HNE-modified proteins was observed in human NASH (fatty) and NASH (not fatty) livers (Figure 4). The IHC staining were then analyzed and quantified. In the normal human liver tissue, only 16% of the area is stained with positive 4-HNE protein adduct staining. The positive staining area is 43%, 37%, and 56% in steatosis, NASH (fatty), and NASH (not fatty), respectively. (Supplementary Figure 1).

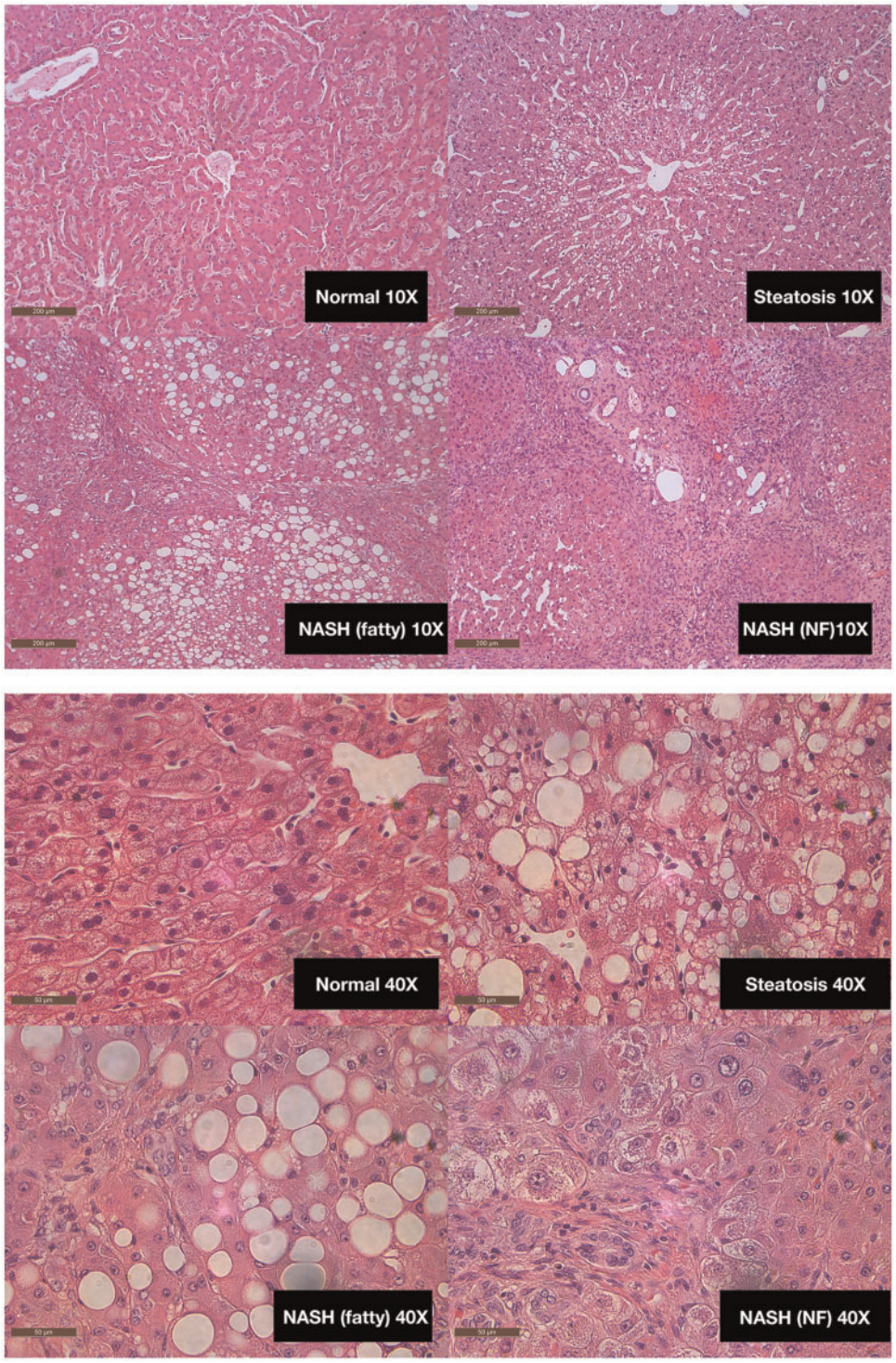

Figure 1. Histology of human livers with progressive stages of NAFLD. H&E-stained human liver slides were examined and scored using NAFLD activity score system. Livers then were identified as normal, steatosis, NASH (fatty) and NASH (not fatty). All of the representative images are shown at 10× magnification and 40× for histopathological features (Normal, $n = 10$; steatosis, $n = 10$; NASH fatty, $n = 10$; NASH not fatty, $n = 10$).

DISCUSSION

Simple steatosis in NAFLD is a relatively mild condition and can be resolved by weight loss, healthy diet, and management of the comorbidities, such as type II diabetes (Schwenger *et al.*, 2018). However, inflammation and fibrosis leads to severe liver injury along with profound global alterations in ADME pathways during NASH (Lake *et al.*, 2011). In this study, the majority of alterations in ADH and ALDH isozymes are found only in NASH, not steatosis. This implies that these enzymes are tightly regulated by a mechanistic feature associated with the irreversible pathological changes in NASH.

In this study, we show no change in the hepatic mRNA expression levels of ADH1A, ADH1B, ADH1C, ADH4, and ADH5

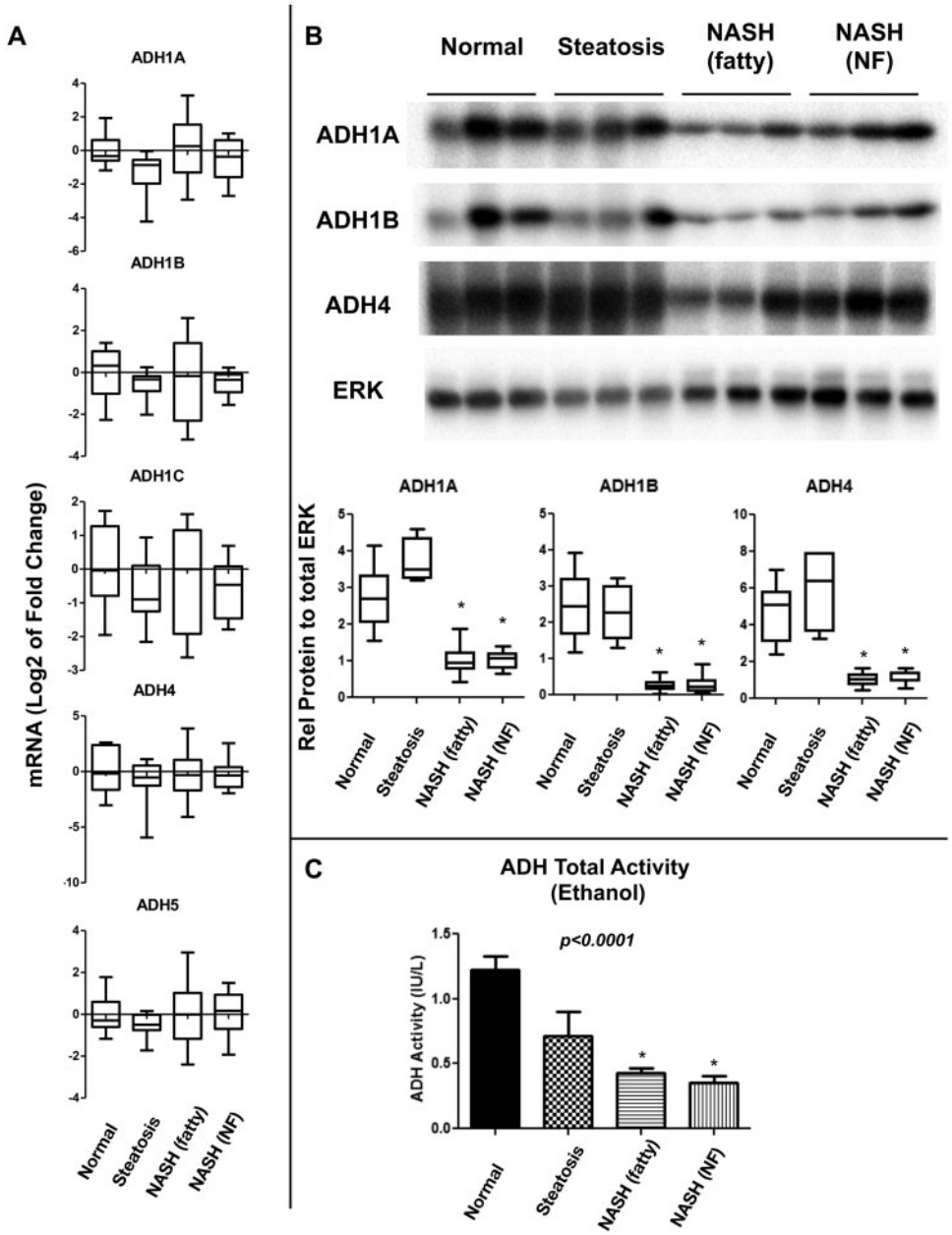

Figure 2. Hepatic expression and function of ADH isoforms during the progression of human NAFLD. A, Relative mRNA content of ADH1A, ADH1B, ADH1C, ADH4, and ADH5 were determined using real-time qPCR. Data are shown in box-whiskers graph (min to max value) (Normal, $n = 10$; steatosis, $n = 10$; NASH fatty, $n = 10$; NASH not fatty, $n = 10$). B, Representative immunoblots of ADH1A, ADH1B, and ADH4 are shown with ERK2 as the loading control. Relative protein levels of all samples were determined by densitometry analysis normalized to ERK2 expression. Data are shown in box-whiskers graph (min to max value). (Normal, $n = 8$; steatosis, $n = 4$; NASH fatty, $n = 11$; NASH not fatty, $n = 7$). C, The overall ADH activity was determined by an ADH activity kit measuring ethanol oxidation. Data represent mean ± SD. Asterisk (*) indicates a significant difference from normal and pound (#) indicated significance from steatosis ($p < .05$).

from patients with progressive stages of NAFLD, (Figure 2A). Interestingly, the protein levels of ADH1A, ADH1B, and ADH4 were significantly decreased in NASH livers (Figure 2B), which indicates that the regulation of ADH genes in human NASH is not controlled at the level of transcription. The ADH isozymes present distinct affinities and catalytic efficiencies in ethanol metabolism, but hepatic metabolism of ethanol is thought to be dominated by class I ADHs, including ADH1A, ADH1B, and ADH1C. In this study, the overall ADH activity measured by ethanol oxidation was significantly decreased in NASH livers (Figure 2C), which is consistent with protein expression. A previous study reported an increase in ADH1C and ADH4 mRNA as well as an increase in ADH1 and ADH4 protein level in pediatric NASH patients (Baker *et al.*, 2010), which contradicts these results. A recent study reported that insulin resistance, which is a critical component in NAFLD progression, could modulate ethanol metabolism in both a mouse model and children with NAFLD. A significantly decreased ADH activity was observed in the insulin resistant mice, which may associate with the increased plasma ethanol concentration in these animals (Engstler *et al.*, 2016).

In addition to ethanol, ADH isozymes are also involved in the metabolism of a variety of endogenous and exogenous substrates, such as retinol, aliphatic alcohols, and lipid aldehydes

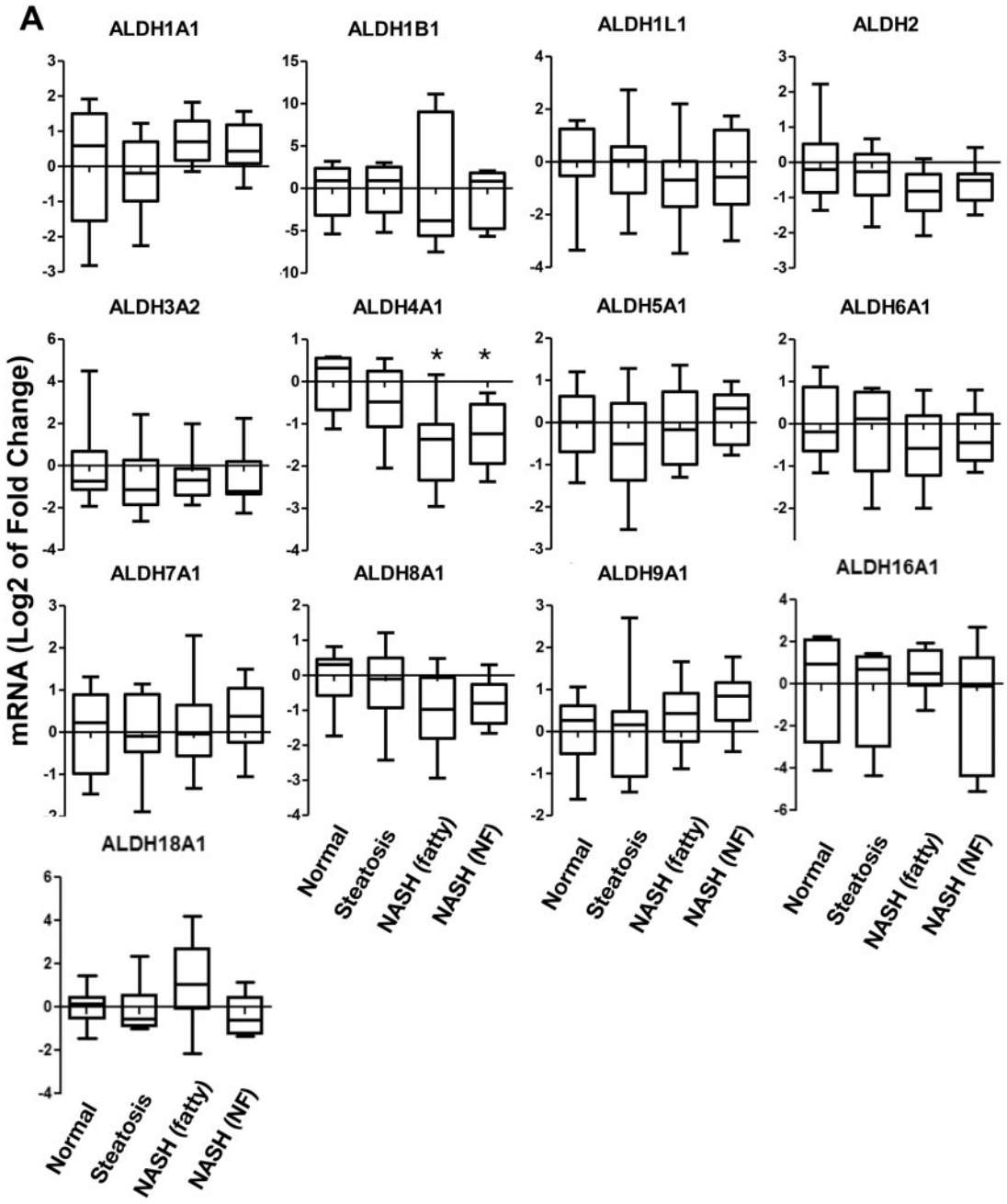

Figure 3. Hepatic expression and function of ALDH isoforms during the progression of human NAFLD. A, Relative mRNA content of were determined using real-time qPCR. ALDH1A1, ALDH1B1, ALDH1L1, ALDH2, ALDH3A2, ALDH4A1, ALDH5A1, ALDH6A1, ALDH7A1, ALDH8A1, ALDH9A1, ALDH16A1, and ALDH18A1 Data are shown in box-whiskers graph (min to max value). (Normal, $n = 10$; steatosis, $n = 10$; NASH fatty, $n = 10$; NASH not fatty, $n = 10$). B, Representative immunoblots of ALDH1A1, ALDH1B1, ALDH2, and ALDH4A1 are shown with ERK2 as the loading control. Relative protein levels of all samples were determined by densitometry analysis normalized to ERK2 expression. Data are shown in box-whiskers graph (min to max value) (Normal, $n = 8$; steatosis, $n = 4$; NASH fatty, $n = 11$; NASH not fatty, $n = 7$). C, The ALDH activity was determined by a ALDH activity kit measuring acetaldehyde, octanal and hexanal oxidation. Data represent mean ± SD. Asterisk (*) indicates a significant difference from normal and pound (#) indicated significance from steatosis ($p < .05$).

(Song *et al.*, 2015). The severity of NAFLD was shown to correlate with a reduction in hepatic but not plasma retinol level (Chaves *et al.*, 2014). However, the reduction of hepatic retinol is attributed to disruption of hepatic retinol storage rather than retinol metabolism (Chen, 2015). The decreased ADH activity in NASH may further reduce the formation of the active metabolites retinal and retinoic acid and may lead to perturbations in retinoic acid mediated cellular signaling and functions. The specific catalytic activity of individual ADH isozymes for retinol metabolism should be further investigated.

In the human ALDH superfamily, there are 19 putatively functional genes with distinct chromosomal locations (Marchitti *et al.*, 2008). The ALDH isozymes have a wide tissue distribution and exhibit distinct substrate specificity. ALDH plays a protective role against cytotoxic aldehydes, including biogenic and lipid peroxidation-derived aldehydes, by oxidizing

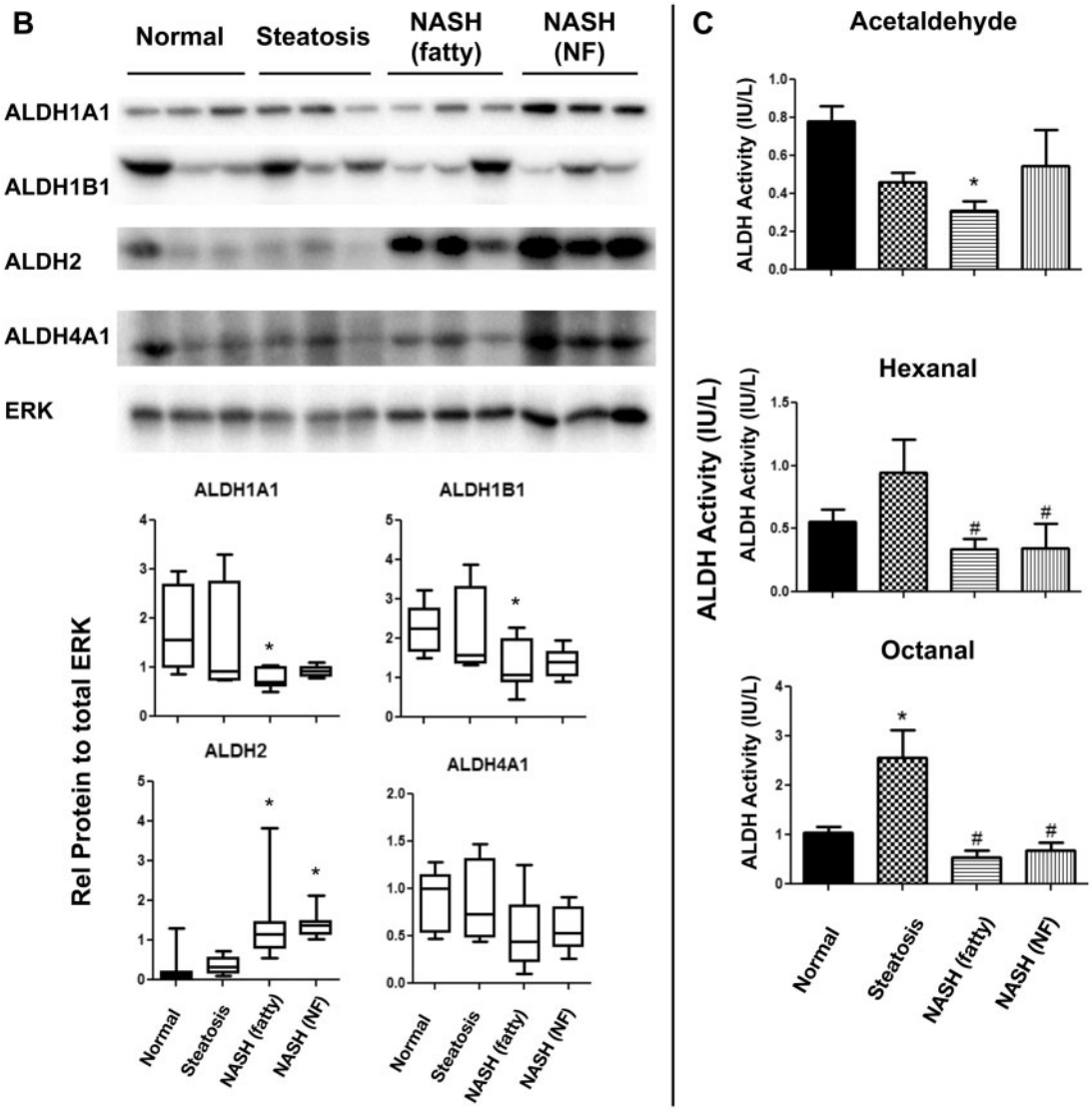

Figure 3. Continued

them to the respective carboxylic acids. A well-known polymorphic ALDH2 variant (ALDH2*2, rs671), which encodes an enzyme with a significantly lower level of activity was recognized as the molecular basis of several disease states and metabolic anomalies (Li *et al.*, 2016; Singh *et al.*, 2013). This study sought to distinguish the effect of the disease on alcohol metabolism from the well-established effect of genetic polymorphisms, therefore individuals carrying the polymorphic allele of ALDH2*2 (rs671) and ADH1B*2 (rs1229984) were excluded from this study to assess the direct impact of NAFLD progression. In this study, we examined 13 hepatic ALDHs, and found a significant decrease only in the ALDH4A1 in NASH (Figure 3A). Unlike ADH, ALDH protein levels were not uniform in response to NAFLD progression. ALDH2 protein level was significantly increased in the NASH groups while ALDH1A1 and ALDH1B1 protein levels were slightly decreased in the NASH (fatty) group (Figure 3B). However, the activity results for these enzymes did not directly correlate to protein data. Decreased overall ALDH activity, measured by acetaldehyde oxidation, was found only in the NASH (fatty) group, while activities against hexanal and octanal were both decreased in the NASH groups compared with simple steatosis, but were not significant from control (Figure 3C). Collectively, these data suggest distinctive regulatory mechanisms in the response to NAFLD pathology for individual ALDH isozymes. The decreased ALDH activity in acetaldehyde metabolism in NASH patients may indicate an impaired acetaldehyde detoxification in these patients and increase their sensitivity to alcohol and alcohol associated toxicity. Posttranslational modifications (PTMs) of ALDH2, as well as the other ALDH isozymes, have been demonstrated to play significant roles in ALDH activities. Multiple PTMs have been found in ALDH enzymes, including oxidation (S-nitrosylation), phosphorylation, nitration, acetylation, methylation, and adduct formation, which can lead to significant alteration in ALDH activity (Song *et al.*, 2011; Song *et al.*, 2014). Chen *et al.* (2008) described the protective effect of ALDH2 activation, which was associated with protein kinase C-mediated ALDH phosphorylation, in ischemic damage to the heart. Conversely, a study by Moon *et al.* reported ALDH2 inhibition by c-Jun N-terminal protein kinase-mediated phosphorylation (Moon *et al.*, 2010). Oxidative modifications on the highly conserved Cys residue within the active site of ALDH2 and other ALDH and suppression of ALDH2 activity were also observed in

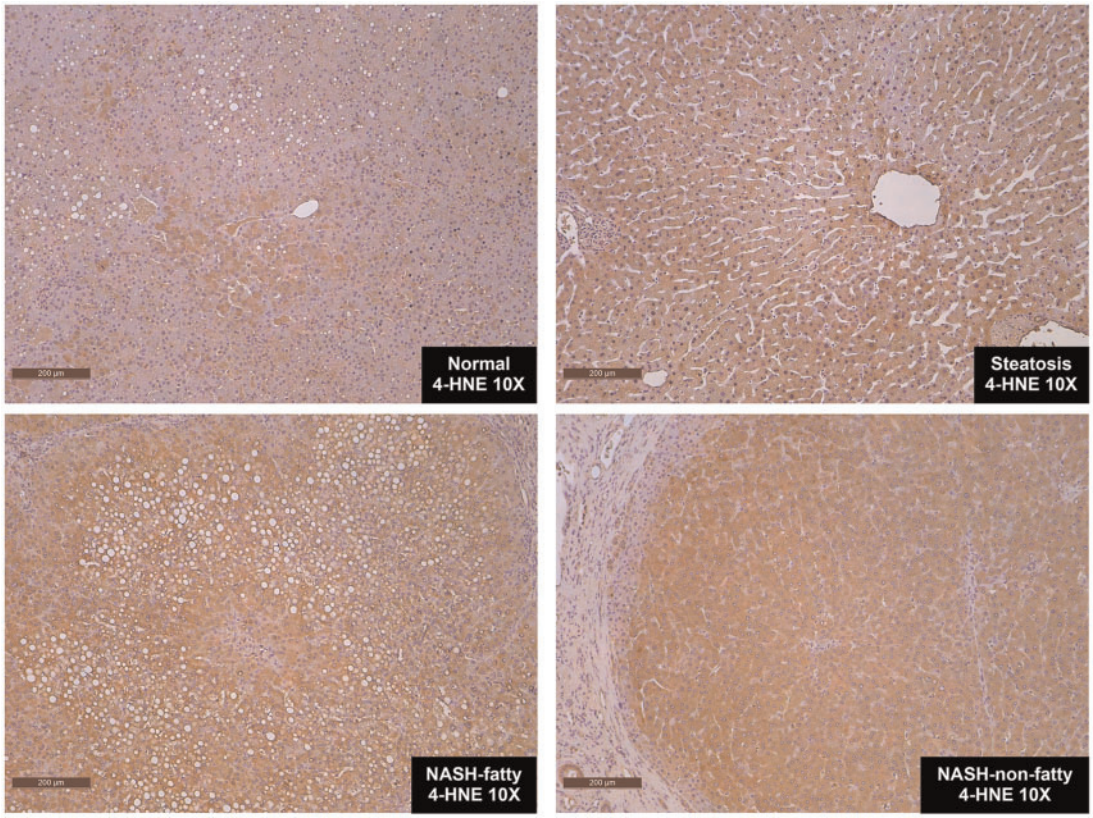

Figure 4. 4-HNE protein adducts formation in human NAFLD progression. IHC staining was performed on formalin-fixed paraffin-embedded liver sections from normal, steatosis, NASH with fatty liver and NASH no longer fatty liver. Tissues were counterstained with hematoxylin and all of the representative images are shown at 10× magnification.

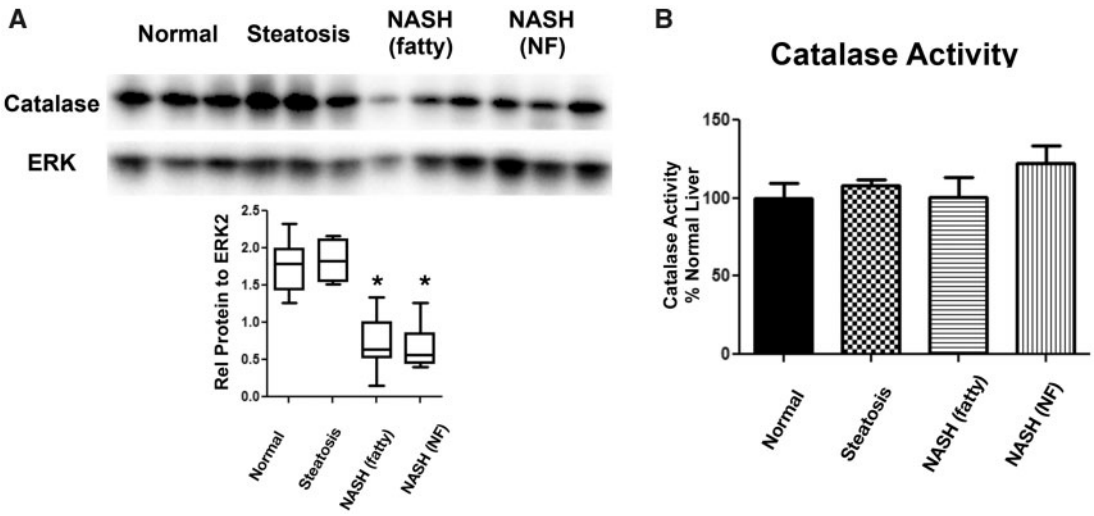

Figure 5. Hepatic expression and function of catalase during the progression of human NAFLD. A, Representative immunoblots of catalase is shown with ERK2 as loading control. Relative protein levels of all samples were determined by densitometry analysis normalized to ERK2 expression. Data are shown in box-whiskers graph (min to max value) (Normal, $n = 8$; steatosis, $n = 4$; NASH fatty, $n = 11$; NASH not fatty, $n = 7$) (B) The catalase activity was determined by a specific catalase activity kit measuring ethanol oxidation. Data represent mean ± SD. Asterisk (*) indicates a significant difference from normal and pound (#) indicated significance from steatosis ($p < .05$).

alcohol-exposed rodents (Moon *et al.*, 2006; Venkatraman *et al.*, 2004). Quantification of IHC staining (Figure 4) indicates a significant accumulation of 4-HNE protein adducts in NASH livers (Figure 4), which indicates significant oxidative stress in NASH. This may also indicate an inadequate ALDH activity in the elimination of 4-HNE. In addition, a covalent modification of ALDH2 active site peptide by 4-HNE was defined by a mass spectral analysis and 4-HNE is reported as an potent irreversible inhibitor of ALDH2 (Doorn *et al.*, 2006). A previous study demonstrated decreased ALDH2 activity in high fat-exposed

diabetic mice, and further characterization revealed that ALDH2 may be inactivated through 4-HNE adduct formation (Mali *et al.*, 2014). Although we do not have direct evidence of ALDH2 inhibition by 4-HNE in human NASH liver, a similar process of lipid peroxide adduct formation could be anticipated. Quantitative proteomics approaches to profile the PTMs on the ALDH during the progression of NASH will further elucidate the regulatory mechanism.

Other than endogenous metabolism, ADH and ALDH also participate in the metabolism of numerous clinical drugs, such as abacavir, torcetrapib, 3-n-butylphthalide, and cyclophosphamide (Dalvie *et al.*, 2008; Diao *et al.*, 2013; Ekhart *et al.*, 2008; Miura and Ohkubo, 2007; Walsh *et al.*, 2002). Therefore, alterations in ADH and ALDH activities may lead to significant changes in the pharmacokinetics of these drugs and introduce potential sources of variable drug responses. As previously demonstrated, the function of individual CYP isoforms are profoundly altered during the progression of NAFLD (Fisher *et al.*, 2009; Li *et al.*, 2017). Since ADH and ALDH work collectively with CYPs in the metabolism of numerous substrates, the resulting pharmacokinetic profile of a given drug may reflect a combination of effects on multiple enzymes. Moreover, the comprehensive interactions of phases I and II metabolizing enzymes and drug transporters in the metabolism and disposition of clinical drugs can significantly increase the complexity in predicting the fate of drugs in NASH patients.

A minor pathway for alcohol metabolism (<10% under normal conditions) is comprised of CYP2E1 and catalase (Lieber, 2005). However, CYP2E1 activity can be significantly induced by alcohol consumption and cause ethanol-induced oxidative stress and mitochondrial toxicity leading to cell injury. CYP2E1 activity is remarkably induced in AFLD (Leung and Nieto, 2013). In a previous study, it has been reported that the CYP2E1 expression and activity in human NASH is not altered (Fisher *et al.*, 2009). Similar to CYP2E1, catalase is considered a minor pathway of alcohol oxidation (Lieber, 2005). A major function of catalase is as an antioxidant enzyme, where it plays a critical role in eliminating ROS and maintaining redox balance. In the current study, protein expression of catalase is significantly decreased in NASH samples, though the *ex vivo* catalase activity remains stable (Figure 5). Since the *in vivo* catalase activity relies on the physiological H_2O_2 concentration, *ex vivo* quantitation may not reflect the physiological catalase activity precisely.

Overall, significant alterations in alcohol metabolizing enzymes were observed in human NASH liver samples. The significant reduction in ADH activity may lead to a reduction in alcohol elimination as well as perturbations in other endogenous metabolism pathways resulting in potential adverse effects in NASH patients. Considering the significant role of ADH and ALDH in drug metabolism, altered ADH and ALDH function may also lead to significant alterations in the pharmacokinetics of substrate drugs and therefore introduce potential variable drug reactions. These data may provide useful information in making appropriate dosing adjustments for NAFLD patients taking drugs that are metabolized by these pathways.

SUPPLEMENTARY DATA

Supplementary data are available at *Toxicological Sciences* online.

FUNDING

This work was supported by National Institutes of Health Grants (HD062489, GM123643, ES007091, ES006694, and P30 CA023074).

REFERENCES

Baker, S. S., Baker, R. D., Liu, W., Nowak, N. J., and Zhu, L. (2010). Role of alcohol metabolism in non-alcoholic steatohepatitis. *PLoS One* **5**, e9570.

Canet, M. J., Merrell, M. D., Hardwick, R. N., Bataille, A. M., Campion, S. N., Ferreira, D. W., Xanthakos, S. A., Manautou, J. E., Hesham A-Kader, H., Erickson, R. P., *et al.* (2015). Altered regulation of hepatic efflux transporters disrupts acetaminophen disposition in pediatric nonalcoholic steatohepatitis. *Drug Metab Dispos*. **43**, 829–835.

Cederbaum, A. I. (2012). Alcohol metabolism. *Clin Liver Dis*. **16**, 667–685.

Chalasani, N., Younossi, Z., Lavine, J. E., Diehl, A. M., Brunt, E. M., Cusi, K., Charlton, M., and Sanyal, A. J. (2012). The diagnosis and management of non-alcoholic fatty liver disease: Practice Guideline by the American Association for the Study of Liver Diseases, American College of Gastroenterology, and the American Gastroenterological Association. *Hepatology* **55**, 2005–2023.

Chaves, G. V., Pereira, S. E., Saboya, C. J., Spitz, D., Rodrigues, C. S., and Ramalho, A. (2014). Association between liver vitamin A reserves and severity of nonalcoholic fatty liver disease in the class III obese following bariatric surgery. *Obes. Surg.* **24**, 219–224.

Chen, C.-H., Budas, G. R., Churchill, E. N., Disatnik, M.-H., Hurley, T. D., and Mochly-Rosen, D. (2008). Activation of aldehyde dehydrogenase-2 reduces ischemic damage to the heart. *Science* **321**, 1493–1495.

Chen, G. (2015). The link between hepatic vitamin A metabolism and nonalcoholic fatty liver disease. *Curr. Drug Targets* **16**, 1281–1292.

Chitturi, S., Abeygunasekera, S., Farrell, G. C., Holmes-Walker, J., Hui, J. M., Fung, C., Karim, R., Lin, R., Samarasinghe, D., Liddle, C., *et al.* (2002). NASH and insulin resistance: Insulin hypersecretion and specific association with the insulin resistance syndrome. *Hepatology* **35**, 373–379.

Clarke, J. D., Hardwick, R. N., Lake, A. D., Lickteig, A. J., Goedken, M. J., Klaassen, C. D., and Cherrington, N. J. (2014). Synergistic interaction between genetics and disease on pravastatin disposition. *J. Hepatol.* **61**, 139–147.

Dalvie, D., Chen, W., Zhang, C., Vaz, A. D., Smolarek, T. A., Cox, L. M., Lin, J., and Obach, R. S. (2008). Pharmacokinetics, metabolism, and excretion of torcetrapib, a cholesteryl ester transfer protein inhibitor, in humans. *Drug Metab. Dispos.* **36**, 2185–2198.

Diao, X., Deng, P., Xie, C., Li, X., Zhong, D., Zhang, Y., and Chen, X. (2013). Metabolism and pharmacokinetics of 3-n-butylphthalide (NBP) in humans: The role of cytochrome P450s and alcohol dehydrogenase in biotransformation. *Drug Metab. Dispos.* **41**, 430–444.

Dinis-Oliveira, R. J. (2016). Oxidative and non-oxidative metabolomics of ethanol. *Curr. Drug Metab.* **17**, 327–335.

Doorn, J. A., Hurley, T. D., and Petersen, D. R. (2006). Inhibition of human mitochondrial aldehyde dehydrogenase by 4-hydroxynon-2-enal and 4-oxonon-2-enal†. *Chem. Res. Toxicol.* **19**, 102–110.

Dzierlenga, A. L., Clarke, J. D., Hargraves, T. L., Ainslie, G. R., Vanderah, T. W., Paine, M. F., and Cherrington, N. J. (2015). Mechanistic basis of altered morphine disposition in nonalcoholic steatohepatitis. *J. Pharmacol. Exp. Ther.* **352**, 462–470.

Ekhart, C., Doodeman, V. D., Rodenhuis, S., Smits, P. H. M., Beijnen, J. H., and Huitema, A. D. R. (2008). Influence of polymorphisms of drug metabolizing enzymes (CYP2B6, CYP2C9, CYP2C19, CYP3A4, CYP3A5, GSTA1, GSTP1, ALDH1A1 and ALDH3A1) on the pharmacokinetics of cyclophosphamide and 4-hydroxycyclophosphamide. *Pharmacogenet. Genomics* **18**, 515–523.

Engstler, A. J., Aumiller, T., Degen, C., Dürr, M., Weiss, E., Maier, I. B., Schattenberg, J. M., Jin, C. J., Sellmann, C., and Bergheim, I. (2016). Insulin resistance alters hepatic ethanol metabolism: Studies in mice and children with non-alcoholic fatty liver disease. *Gut* **65**, 1564–1571.

Evans, W. E., and Relling, M. V. (1999). Pharmacogenomics: Translating functional genomics into rational therapeutics. *Science* **286**, 487–491.

Fisher, C. D., Lickteig, A. J., Augustine, L. M., Ranger-Moore, J., Jackson, J. P., Ferguson, S. S., and Cherrington, N. J. (2009). Hepatic cytochrome P450 enzyme alterations in humans with progressive stages of nonalcoholic fatty liver disease. *Drug Metab. Dispos.* **37**, 2087–2094.

Glorieux, C., and Calderon, P. B. (2017). Catalase, a remarkable enzyme: Targeting the oldest antioxidant enzyme to find a new cancer treatment approach. *Biol. Chem.* **398**, 1095–1108.

Gonzalez-Rodriguez, A., Mayoral, R., Agra, N., Valdecantos, M. P., Pardo, V., Miquilena-Colina, M. E., Vargas-Castrillon, J., Lo Iacono, O., Corazzari, M., Fimia, G. M., *et al.* (2014). Impaired autophagic flux is associated with increased endoplasmic reticulum stress during the development of NAFLD. *Cell Death Dis.* **5**, e1179.

Han, J., Dzierlenga, A. L., Lu, Z., Billheimer, D. D., Torabzadeh, E., Lake, A. D., Li, H., Novak, P., Shipkova, P., Aranibar, N., *et al.* (2017). Metabolomic profiling distinction of human nonalcoholic fatty liver disease progression from a common rat model. *Obesity* **25**, 1069–1076.

Hardwick, R. N., Clarke, J. D., Lake, A. D., Canet, M. J., Anumol, T., Street, S. M., Merrell, M. D., Goedken, M. J., Snyder, S. A., and Cherrington, N. J. (2014). Increased susceptibility to methotrexate-induced toxicity in nonalcoholic steatohepatitis. *Toxicol. Sci.* **142**, 45–55.

Hardwick, R. N., Ferreira, D. W., More, V. R., Lake, A. D., Lu, Z., Manautou, J. E., Slitt, A. L., and Cherrington, N. J. (2013). Altered UDP-glucuronosyltransferase and sulfotransferase expression and function during progressive stages of human nonalcoholic fatty liver disease. *Drug Metab. Dispos.* **41**, 554–561.

Hardwick, R. N., Fisher, C. D., Canet, M. J., Scheffer, G. L., and Cherrington, N. J. (2011). Variations in ATP-binding cassette transporter regulation during the progression of human nonalcoholic fatty liver disease. *Drug Metab. Dispos.* **39**, 2395–2402.

Lake, A. D., Novak, P., Fisher, C. D., Jackson, J. P., Hardwick, R. N., Billheimer, D. D., Klimecki, W. T., and Cherrington, N. J. (2011). Analysis of global and absorption, distribution, metabolism, and elimination gene expression in the progressive stages of human nonalcoholic fatty liver disease. *Drug Metab. Dispos.* **39**, 1954–1960.

Lake, A. D., Novak, P., Hardwick, R. N., Flores-Keown, B., Zhao, F., Klimecki, W. T., and Cherrington, N. J. (2014). The adaptive endoplasmic reticulum stress response to lipotoxicity in progressive human nonalcoholic fatty liver disease. *Toxicol. Sci.* **137**, 26–35.

Leung, T.-M., and Nieto, N. (2013). CYP2E1 and oxidant stress in alcoholic and non-alcoholic fatty liver disease. *J. Hepatol.* **58**, 395–398.

Li, H., Canet, M. J., Clarke, J. D., Billheimer, D., Xanthakos, S. A., Lavine, J. E., Erickson, R. P., and Cherrington, N. J. (2017). Pediatric cytochrome P450 activity alterations in nonalcoholic steatohepatitis. *Drug Metab. Dispos.* **45**, 1317.

Li, R., Zhao, Z., Sun, M., Luo, J., and Xiao, Y. (2016). ALDH2 gene polymorphism in different types of cancers and its clinical significance. *Life Sci.* **147**, 59–66.

Lieber, C. S. (2005). Metabolism of alcohol. *Clin. Liver Dis.* **9**, 1–35.

Mali, V. R., Ning, R., Chen, J., Yang, X.-P., Xu, J., and Palaniyandi, S. S. (2014). Impairment of aldehyde dehydrogenase-2 by 4-hydroxy-2-nonenal adduct formation and cardiomyocyte hypertrophy in mice fed a high-fat diet and injected with low-dose streptozotocin. *Exp. Biol. Med. (Maywood)* **239**, 610–618.

Marchitti, S. A., Brocker, C., Stagos, D., and Vasiliou, V. (2008). Non-P450 aldehyde oxidizing enzymes: The aldehyde dehydrogenase superfamily. *Expert Opin. Drug Metab. Toxicol.* **4**, 697–720.

Miura, M., and Ohkubo, T. (2007). Identification of human cytochrome P450 enzymes involved in the major metabolic pathway of fluvoxamine. *Xenobiotica* **37**, 169–179.

Moon, K.-H., Hood, B. L., Kim, B.-J., Hardwick, J. P., Conrads, T. P., Veenstra, T. D., and Song, B. J. (2006). Inactivation of oxidized and S-nitrosylated mitochondrial proteins in alcoholic fatty liver of rats. *Hepatology* **44**, 1218–1230.

Moon, K.-H., Lee, Y.-M., and Song, B.-J. (2010). Inhibition of hepatic mitochondrial aldehyde dehydrogenase by carbon tetrachloride through JNK-mediated phosphorylation. *Free Radic. Biol. Med.* **48**, 391–398.

Schwenger, K. J. P., Fischer, S. E., Jackson, T. D., Okrainec, A., and Allard, J. P. (2018). Non-alcoholic fatty liver disease in morbidly obese individuals undergoing bariatric surgery: Prevalence and effect of the pre-bariatric very low calorie diet. *Obes. Surg.* **28**(4), 1109–1116.

Singh, S., Brocker, C., Koppaka, V., Chen, Y., Jackson, B. C., Matsumoto, A., Thompson, D. C., and Vasiliou, V. (2013). Aldehyde dehydrogenases in cellular responses to oxidative/electrophilic stress. *Free Radic. Biol. Med.* **56**, 89–101.

Song, B.-J., Abdelmegeed, M. A., Yoo, S.-H., Kim, B.-J., Jo, S. A., Jo, I., and Moon, K.-H. (2011). Post-translational modifications of mitochondrial aldehyde dehydrogenase and biomedical implications. *J. Proteomics* **74**, 2691–2702.

Song, B.-J., Akbar, M., Abdelmegeed, M. A., Byun, K., Lee, B., Yoon, S. K., and Hardwick, J. P. (2014). Mitochondrial dysfunction and tissue injury by alcohol, high fat, nonalcoholic substances and pathological conditions through post-translational protein modifications. *Redox. Biol.* **3**, 109–123.

Song, B.-J., Akbar, M., Jo, I., Hardwick, J. P., and Abdelmegeed, M. A. (2015). Translational implications of the alcohol-metabolizing enzymes, including cytochrome P450-2E1, in alcoholic and nonalcoholic liver disease. *Adv. Pharmacol.*, **74**, 303–372.

Strolin Benedetti, M., Whomsley, R., and Baltes, E. (2006). Involvement of enzymes other than CYPs in the oxidative metabolism of xenobiotics. *Expert Opin. Drug Metab. Toxicol.* **2**, 895–921.

Takaki, A., Kawai, D., and Yamamoto, K. (2013). Multiple hits, including oxidative stress, as pathogenesis and treatment

target in non-alcoholic steatohepatitis (NASH). *Int. J. Mol. Sci.* **14**, 20704–20728.

Vasiliou, V., Pappa, A., and Estey, T. (2004). Role of human aldehyde dehydrogenases in endobiotic and xenobiotic metabolism. *Drug Metab. Rev.* **36**, 279–299.

Venkatraman, A., Landar, A., Davis, A. J., Ulasova, E., Page, G., Murphy, M. P., Darley-Usmar, V., and Bailey, S. M. (2004). Oxidative modification of hepatic mitochondria protein thiols: Effect of chronic alcohol consumption. *Am. J. Physiol. Gastrointest. Liver Physiol.* **286**, G521–G527.

Vernon, G., Baranova, A., and Younossi, Z. M. (2011). Systematic review: The epidemiology and natural history of non-alcoholic fatty liver disease and non-alcoholic steatohepatitis in adults. *Aliment. Pharmacol. Ther.* **34**, 274–285.

Walsh, J. S., Reese, M. J., and Thurmond, L. M. (2002). The metabolic activation of abacavir by human liver cytosol and expressed human alcohol dehydrogenase isozymes. *Chem. Biol. Interact.* **142**, 135–154.

Younossi, Z. M., Koenig, A. B., Abdelatif, D., Fazel, Y., Henry, L., and Wymer, M. (2016). Global epidemiology of nonalcoholic fatty liver disease—Meta-analytic assessment of prevalence, incidence, and outcomes. *Hepatology* **64**, 73–84.